# Magnetoquasistatic Tracking of an American Football: A Goal Line Measurement

Darmindra D. Arumugam, *Member, IEEE*, Joshua D. Griffin, *Member, IEEE*, Daniel D. Stancil, *Fellow, IEEE*, and David S. Ricketts, *Member, IEEE*

**Abstract**

An American football is tracked using a long-range magnetoquasistatic position and orientation measurement system. A low-weight emitter that emits a low-frequency quasistatic magnetic field is embedded within an American football. The emitter weighs a total of 26.5 g, which is within the manufacturing tolerance of an American football, and does not alter the dynamics of the ball. Measurements of a person carrying the football along the goal line of an American football field is described, along with a description of the construction of the magnetoquasistatic tracking system. The technique demonstrates measurements with a distance accuracy of 15 cm and an azimuthal orientation accuracy of 2.45° for measurements conducted along the goal line of an American football field.

**Index Terms**

Electromagnetic fields, magnetoquasistatics, radio position measurement, radio tracking.

## I. Introduction

In this work, we report on a non-line-of-sight (NLoS) position tracking system for sports visualization. Sports visualization has become an important aspect of both the perception of sporting events as well as in accurately tracking play. In American football, tracking the location of the football is exceedingly difficult due to the presence of 22 players in close proximity to the ball. In fact, during the most controversial plays, the football is often partially, or totally obscured by one or more players.

Our solution is to use low-frequency, magnetoquasistatic fields to sense the ball's location and orientation [1], [2]. Objects that are weakly conducting and are small in size compared to the equivalent skin depth at the frequency of operation, such as the human body, are essentially transparent to low-frequency fields [3]. Moreover, the non-propagating nature of magnetoquasistatic fields removes the often problematic issue of scattering and multi-path interference present in many propagation-based position tracking techniques, e.g. RF-identification (RFID) systems.

To illustrate our approach and its potential impact, we present experimental results of a football tracking experiment, where the football is carried by a person along the goal line. This experiment illustrates the tracking capability when the ball is obstructed by a person as well as the present accuracy of this approach. We show that an American football, with an integrated tracking transmitter, can be tracked with an average distance accuracy of 15 cm and azimuthal orientation accuracy of 2.45° along the goal line.

## II. Magnetoquasistatic Positioning Technique using Complex Image Theory

The theory and concept of magnetoquasistatic positioning has been reported in [1]. We briefly review this approach for completeness and also to establish an understanding for the measurement described in this work.

The long-range magnetoquasistatic position tracking approach described in this work uses low-frequency magnetoquasistatic fields with wavelengths on the order of many hundred's of meters, which correspond to frequencies on the order of hundred's of kilohertz [1]. The approach is to use a frequency that provides a quasistatic range that covers the region of operation while providing adequate signal-to-noise ratio (SNR). For the purpose of tracking an American football, we required a quasistatic region of greater than 50 m, which corresponds to the width of the football field. We found that a frequency of approximately 400 kHz provided the sufficient SNR and quasistatic range while avoiding interference with AM-band signals.

Due to the use of magnetoquasistatic fields, both the emitter and receiver use a loop antenna to preferentially excite and detect magnetic fields as shown in Fig. 1. Because the emitter is electrically-close to the earth, the measured magnetic field of the emitting current loop in proximity to the ground can be decomposed into the field of the loop and the induced eddy-currents in the ground [4]. Experiments have verified that complex image theory accurately models the secondary field due to the induced-eddy currents in the ground [1]. The total magnetic field outside the ground is given by:

D. D. Arumugam was with the Department of Electrical and Computer Engineering, Carnegie Mellon University, Pittsburgh, PA, 15213. He is currently with Jet Propulsion Laboratory, California Institute of Technology, Pasadena, CA, 91109 USA e-mail: darmindra.d.arumugam@jpl.nasa.gov.

J. D. Griffin is with Disney Research Pittsburgh, Pittsburgh, PA, 15213 USA e-mail: joshdgriffin@disneyresearch.com.

D. D. Stancil is with the Department of Electrical and Computer Engineering, North Carolina State University, Raleigh, NC, 27695 USA e-mail: ddstancil@ncsu.edu.

D. S. Ricketts is with the Department of Electrical and Computer Engineering, North Carolina State University, Raleigh, NC, 27695 e-mail: david.ricketts@ncsu.edu.

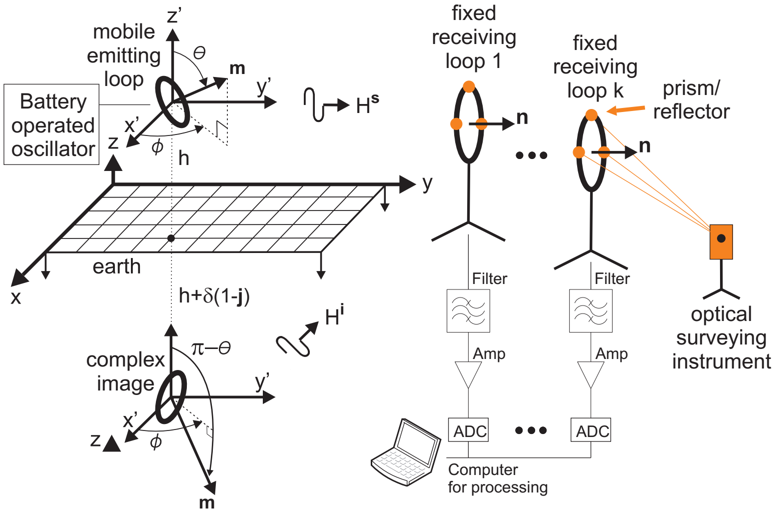


Fig. 1. The magnetoquasistatic technique. The magnetic field emitted by a battery operated oscillator is detected at multiple receivers located around the field. Complex image theory is used to account for secondary fields due to induced eddy-currents in the ground. An optical surveying instrument is used to measure receiver position and orientations.

$$H_p(x,y,z) = \vec{H}^d(x,y,z-h) + c_p\vec{H}^d(x,y,-z-\alpha), \tag{1}$$

where $p = ||, \perp$ describes fields parallel and perpendicular to the ground, $c_{||} = 1$ and $c_\perp = -1$, $\alpha = h + \delta(1-j)$, $\delta$ is the skin depth, and $\vec{H}^d$ is the dipole field given by [5]:

$$\vec{H}^d(x,y,z) = \frac{1}{4\pi}\left[\frac{3\vec{r}(\vec{m}\cdot\vec{r}) - \vec{m}r^2}{r^5}\right], \tag{2}$$

where $\vec{m}$ is the moment and $\vec{r}$ is the position vector from the origin to observation. The theoretical description of the voltage at the terminals of any receiver shown in Fig. 1 is given by:

$$V^T = -j\omega\mu_o\left[\hat{n}\cdot\left(\vec{H_{||}} + \vec{H_\perp}\right)\right]a, \tag{3}$$

where $\hat{n}$ is the unit vector normal to the receive loop and $a$ is the surface area of the loop. Use of $k$ fixed receivers with known positions and orientations, as shown in Fig. 1, generates a set of $k$ equations from which the emitter's unknown position and orientation can be found. This is done by minimizing the sum of squared difference between the measured voltage ($V^M$) at the terminal of each loop and the expression in (3):

$$\Phi = \sum_{i=1}^{k}\left[V_i^T - V_i^M\right]^2, \tag{4}$$

using a numerical, nonlinear, least-square optimization algorithm. We employ a trust-region reflective optimization algorithm [6]. This algorithm generates lower-dimensional trust-regions, within which trial steps are used to force global convergence via the steepest descent direction. Local convergence is found using the Newton step. The algorithm is effective on sparse problems.

## III. Football Tracking System and Measurement Setup

The system concept is illustrated in Fig. 1. Here, the emitting loop is fed a 360.6 kHz signal using a battery operated oscillator. The generated field is measured at multiple receivers located outside the measurement zone, in this case the football field. An optical surveying instrument is used to determine the precise position and orientation of each receiver, which is required to solve for the position and orientation of the emitter, which is embedded in the American football.

The emitter is integrated into the football and is composed of a 50-turn coil [34 American Wire Gauge (AWG) wire] driven by a class-E oscillator circuit [7], with power supplied through a rechargeable coil-cell battery, as shown in Fig. 2a. Figure 2b shows a photo of the emitter circuit after fabrication and population. This integration is shown in Fig. 2c-d. The loop is wrapped around the football such that the axis of the ball is aligned with the surface normal vector of the loop. Figure 2e shows a completely integrated football with built-in circuit and battery.

The receiver setup described by Fig. 1 shows three optical reflectors used to determine the exact location and orientation of the receive antennas. Figure 2f shows the actual antenna (model LFL-1010 by Wellbrook Communications) on a tripod. The

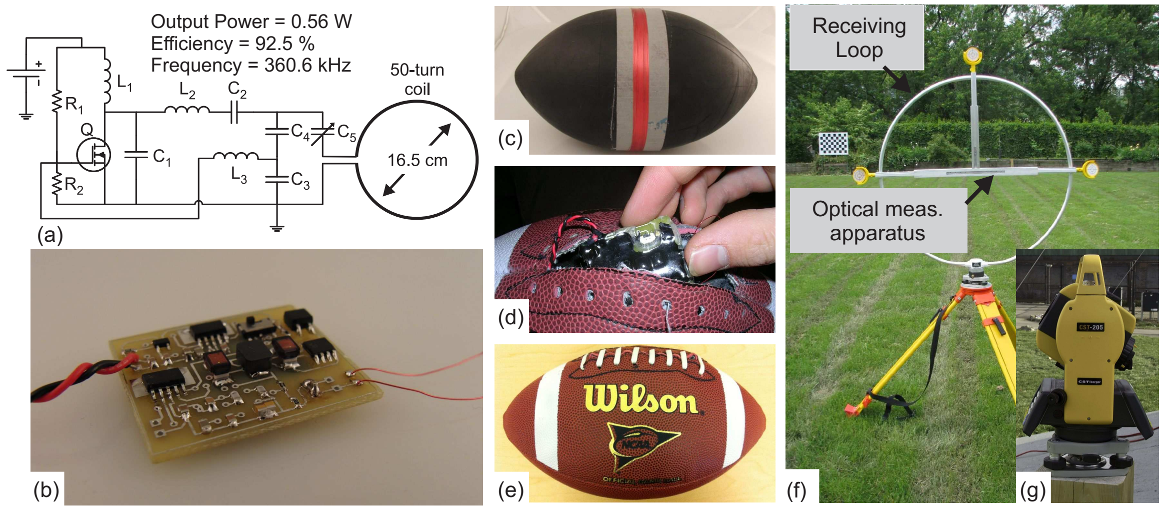


Fig. 2. The emitter circuit design using a class-E oscillator is shown in (a). The fabricated and populated circuit board is shown in (b). The loop and circuit integration into the American football is shown in (c) and (d). The completely integrated football is shown in (e). The receiving loop along with the optical measurements apparatus and three reflectors are shown in (f). The optical surveying instrument is shown in (g).

reflectors shown are held by an apparatus that is removed prior to any RF measurements. Because the receivers are not moved during the measurements, only a single ground truth measurement is necessary, which is conducted prior to RF measurements. The optical surveying instrument (CST205 manufactured by CST/Berger) with built-in electronic distance measurement is shown in Fig. 2g.

The magnetic field generated by the emitter induces a voltage at the terminals of each receiving loop positioned outside the football field (Fig. 1). The RF receiver system used to detect this voltage is shown in Fig. 3. For each receiver system, an active receiving loop with a diameter of 1 m, a band-pass filter to attenuate unwanted signals such as AM broadcast bands and low-frequency maritime radio beacons (bandpass region of 300 kHz to 450 kHz), and an ultra-low-noise amplifier (AD8331 by Analog Devices) are used. The received signals are digitized using a 16-bit 10 MS/s analog-to-digital converter (ADC) included in the PXI-9816D/512 digitizer by Adlink Technologies. A voltage range of $\pm$ 0.2V is used during the football field measurements.

The long coaxial cables used to connect the receiving loop antennas, distributed around the football field (to the digitizer/ADC), can themselves receive significant signals from the emitter. To reduce the effect of cable coupling, the loop amplification block in Fig. 3 is placed directly after the terminals of the receiving loop. This amplifies the signal at the terminals of the receiving loop such that the signal becomes much larger than any signal induced on the long cables, resulting in improved signal-to-noise plus interference (SNIR) ratio at the ADC. DC power is supplied to the active receiving loop and the loop amplification block through a series of bias-tee's shown within both the RF/DC block and loop amplification block of Fig. 3. The receiver system described in Fig. 3 is used for each receiving loop. The gain and losses of each RF link were measured individually and used to calibrate the measured voltage at the terminals of the loops.

The measurement setup used on the football field is shown in Fig. 4. The measurement was conducted in the Gesling football stadium at Carnegie Mellon University on September 2, 2011. Figure 4a shows a close-up view of the electronics and optical system setup during the measurements. One of the authors, D. Arumugam, is shown initiating a capture sequence to obtain

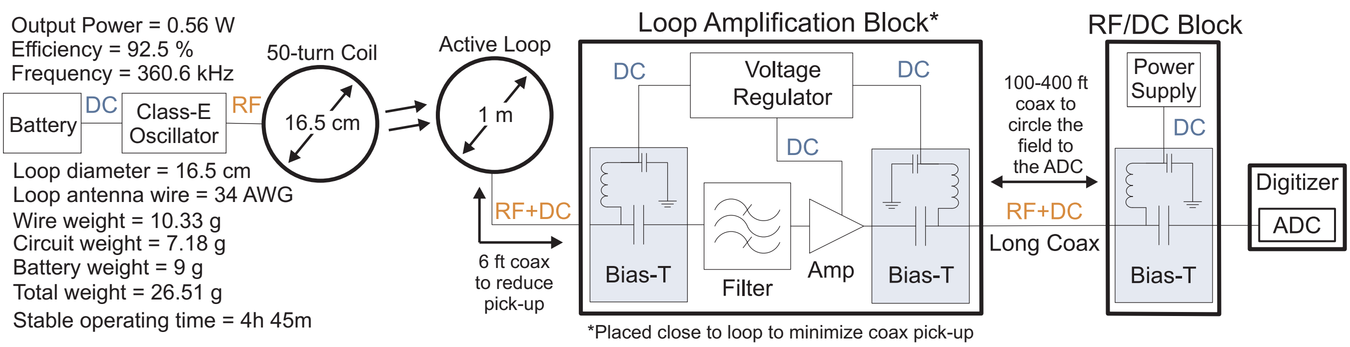


Fig. 3. RF block diagram for the emitter and for a single receiver channel. The loop amplification block is located near the receiving loop, whereas the RF/DC block is located outside the field near. The emitter weight a total of 26.5 g, which is within the manufacturing tolerance of the American football (28 g). It is designed to have a stable operating time of approximately 4h 45m.

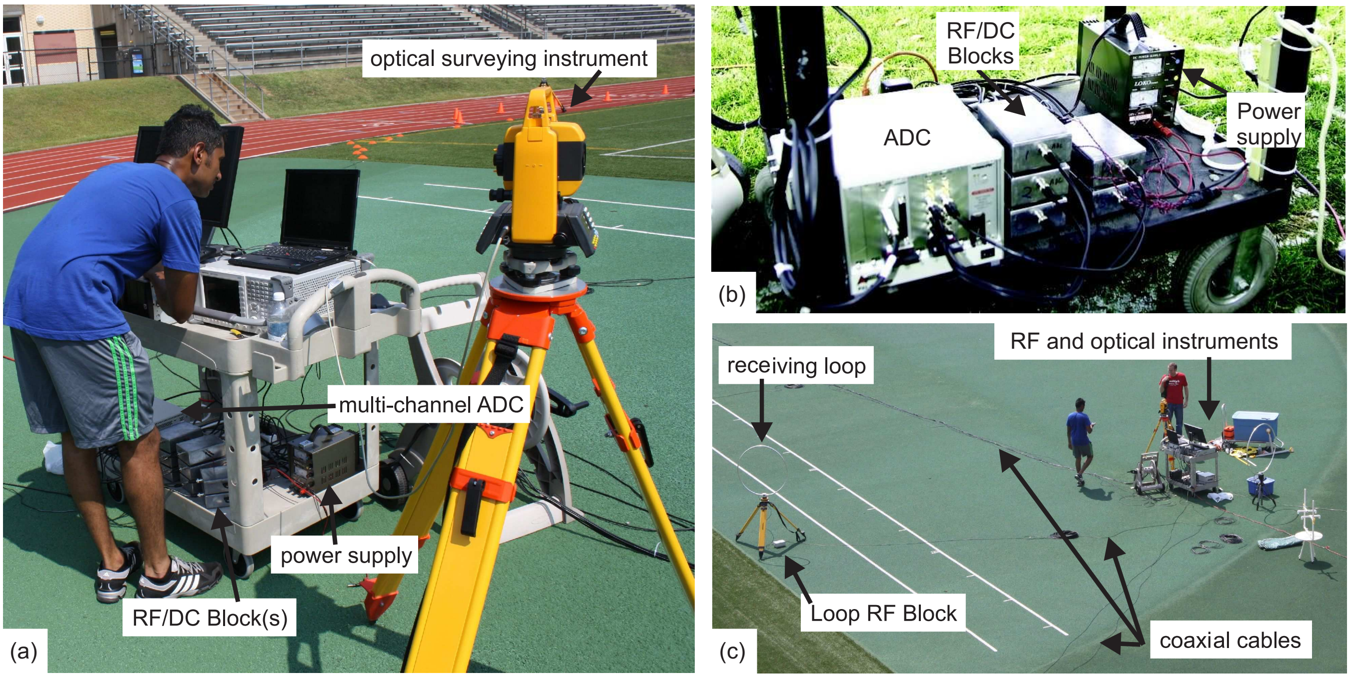


Fig. 4. One of the authors, D. Arumugam, is shown operating the RF electronics during the measurement day (a). The RF instruments designed (except the loop amplification block) is shown in the bottom of the cart in (a), or in the close-up (modified from [2]) as shown in (b). A top view for the setup of the measurement electronics, placed outside the football field, can be seen in (c). The loop seen on the left of (c) is one of eight loops used in the measurements.

time-domain data from the multi-channel ADC. A majority of the RF electronics described in Fig. 3 are located at the bottom shelf of the measurement cart, excluding the loop amplification box which is located near each receiver. A photo of the setup for the RF instruments in the bottom shelf of Fig. 4a is shown in Fig. 4b. Figure 4c shows a top view of the electronics and optical system setup during the measurements. The electronics and optical system are positioned outside the usable portion of the football field and the coaxial cables are routed to each loop amplification block and receiver.

A total of eight receiving loops were used in the configuration shown in Fig. 5. The purpose was to target measurements within the region covering the 20 yard line to the end-zone of the football field. Receiving loops were located along the 10 yard and 0 yard (goal line), and outside the football field, as well as in the end-zone. The loops located in the end-zone were distributed along the width of the field. The inset figure in Fig. 5 shows a close-up view of a receiver, where the loop amplification block is visible on the ground.

## IV. Football Field Measurement and Results

We used a goal line test to determine the distance and azimuthal orientation accuracy of the positioning system when the American football was in motion. The football was oriented such that the axis of the ball, or normal of the emitting loop, was parallel to the direction of motion along the goal line. In this test, a person holds the ball in this manner and walks along the goal line. The measure of distance accuracy will be determined by the distance of the solved location from the goal line. The measure of azimuthal orientation accuracy will be determined by the difference between the anticipated azimuthal orientation and measured orientation. The error is obtained by measuring the goal line end-points using optical instrumentation prior to the measurement to obtain a measure of expected position and orientation from the RF measurements. Because it is not possible to obtain optical measurements of the ball in motion, we are only able to determine the spatial deviation of the ball from the goal line and the angular deviation of the azimuthal orientation from the expected orientation relative to the goal line.

The measurement conducted and shown in Fig. 5 was that of a person walking on the goal line, where the path traversed is represented explicitly by the dashed blue lines. The person walks along the measurement route a total of three times without any breaks. An ADC data capture window duration of 5 ms was used. The measurement system was configured to loop over the period of the measurement. We achieved an update rate of 35 Hz for the 5 ms sampling window on all eight channels simultaneously using a desktop computer running the commercial software Matlab by Mathworks [8]. This update rate allowed us to collect and record data while the football/emitter was in motion. For each 5 ms measurement window, the time-domain data sampled by the ADC is converted into a frequency-domain spectrum using a Fast Fourier Transform (FFT) algorithm. For each receive channel, the peak voltage at approximately 360.6 kHz was captured and stored for processing using the technique described in Section II. Because the receiver position and orientations were known a-priori through optical measurements, the 5 ms measurement window was used to obtain eight unique measure's of received voltage from the eight receiving loops. From

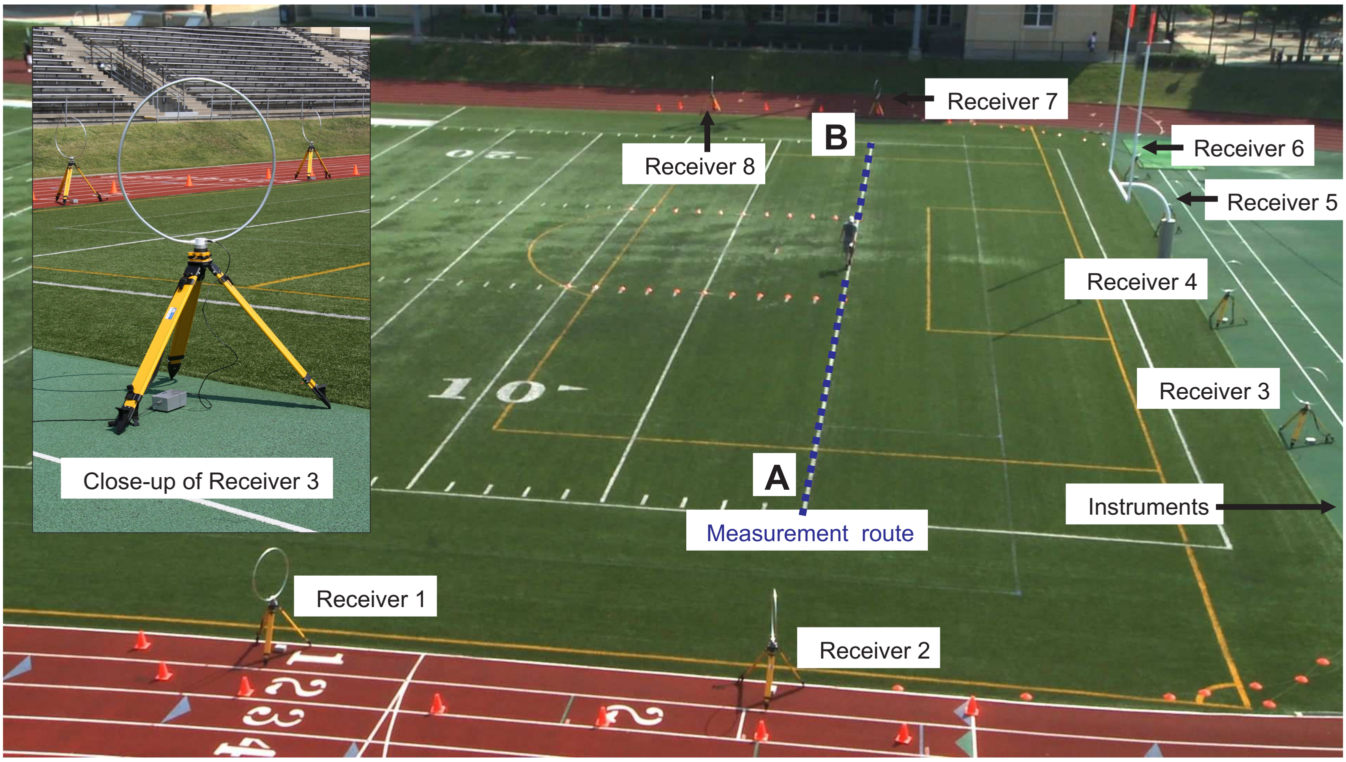


Fig. 5. Top view of the measurement setup on the football field. The RF electronics and optical instruments are located outside usable area of the football field and on the right. Eight receivers are used for the measurements. The receivers were located outside the field and concentrated within the 20 yard line of the football field. A person held the ball while traversing the measurement route (goal line) shown.

these eight unique voltage measurements, the position and orientation of the emitter was found using (1)-(4) after correcting the measured voltages for gains/losses in each RF link.

Figure 6a shows the estimated distance error from the goal-line, obtained from the magnetoquasistatic positioning technique and system. The result in Fig. 6a is obtained by optically measuring the end-points of the goal line and calculating the distance from the solved two-dimensional ($x$ and $y$, but not $z$) position to the closest point on the goal line. The horizontal axis of Fig. 6a denotes each 5 ms measurement window. As mentioned earlier, the person holding the ball walks along the measurement path a total of three times without any breaks. To accomplish this, the person walks starting from point A to B, then B to A, and finally from A to B in Fig. 5. Figure 6b shows a histogram of the distance error found in Fig. 6a. A bin size of 5 cm is used in the histogram. A mode of 10 cm is observed for distance error to the goal line from the measurement results. A cumulative distribution function (CDF) of the measurement results is shown in Fig. 6c. From these results, we see that besides a few outliers, the majority of the results show an error of less than 50 cm with a strong concentration within the 10-25 cm region. The measurements resulted in an average distance error of 15 cm. There appeared to be some systematic errors that appeared at the same location for the 3 walks from A/B to B/A. We believe these are likely due to fixed field/instrumentation induced errors and can be eliminated with proper calibration in the future to reduce the overall average error even further. There were also random errors due to measurement noise, and due to uncertainty in the accuracy of the position and orientation of the football held by the person, i.e., caused by human error. Based on the result of the measurements, we expect the human error to be lesser than the random error due to measurement noise.

During the measurements, the azimuthal orientation of the axis of the football was held in the direction parallel to motion. Due to knowledge of the goal line geometry from optical measurements, the azimuthal orientation of the axis of the football, or surface normal unit vector of the emitting loop, relative to the goal-line can be obtained from measurements. Figure 7a shows the measured azimuthal orientation of the axis of the football from the goal-line, obtained from the magnetoquasistatic positioning technique and system. The results show that the azimuthal orientation is approximately -90° and +90° from the direction perpendicular to the goal line, for direction A-B and B-A in Fig. 5, respectively. The highlighted areas in Fig. 7a indicates transition regions at location A or B where the person and football undergoes rotation. As before, the horizontal axis of Fig. 7a denotes each 5 ms measurement window. Figure 7b shows the absolute value of the result in Fig. 7a. The purpose here is to enable a close-up view of the variation about the expected azimuthal orientation of $\pm 90°$. Figure 7c shows the estimated azimuthal error, found by taking the difference between the result in Fig. 7b and the expected azimuthal orientation of $\pm 90°$. Figure 7d shows a histogram of the azimuthal orientation error found in Fig. 7c. A bin size of 0.25° is used in the histogram. A mode of 1.25° is observed for azimuthal orientation error from the orientation of the goal line. A cumulative

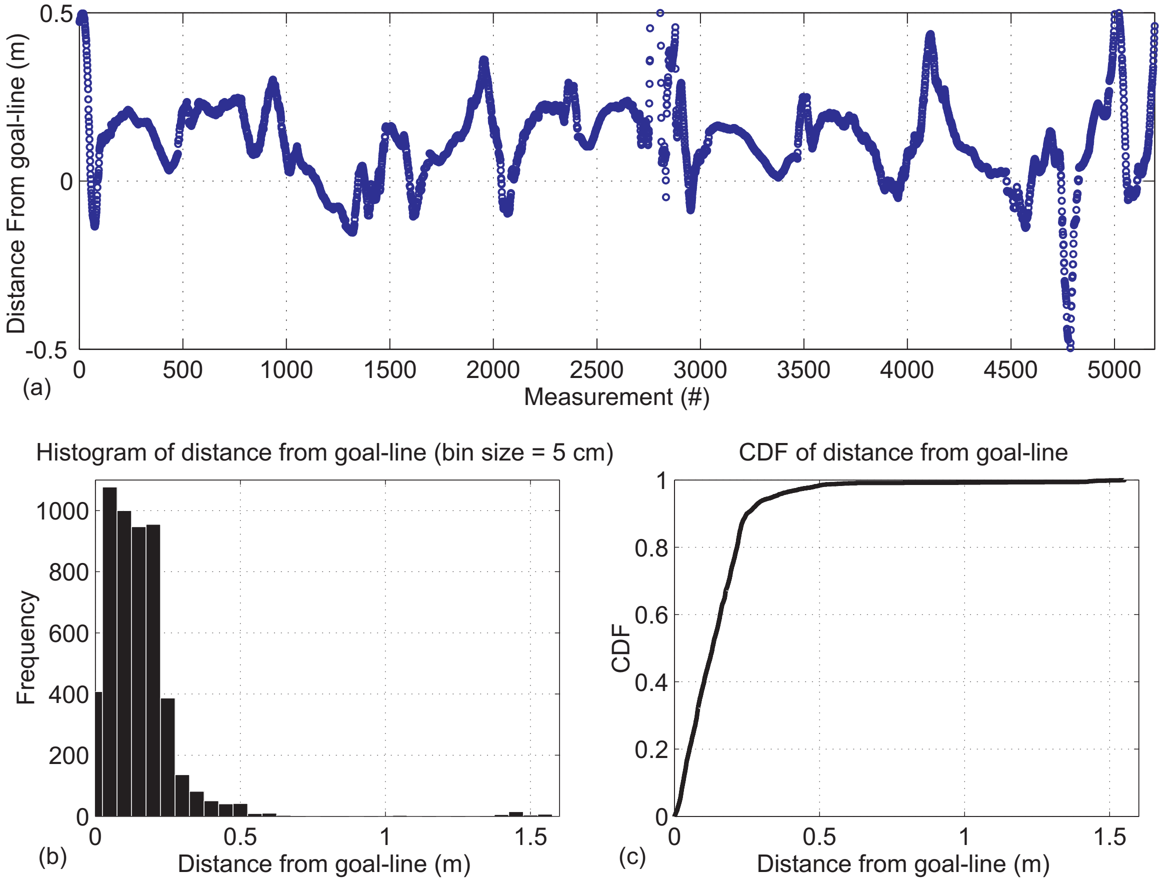


Fig. 6. Distance error from the goal line (a), obtained by finding the distance between the solved position and the goal line. A histogram of the distance error is shown in (b). A CDF of the distance error is shown in (c).

distribution function (CDF) of the measurement results is shown in Fig. 7e. From these results, we see that besides a few outliers, the majority of the results show an error of less than 5° with a strong concentration within the 1-4° region. The measurements resulted in an average azimuthal orientation error of 2.45°.

## V. Conclusion

In this paper we demonstrated a long-range magnetoquasistatic system for position and orientation determination of an American football during game-play. The system is shown to track the American football when the football was in motion. The measurements were conducted on a football field, and all RF receiver systems were located outside the field. We demonstrated a distance accuracy of 15 cm and an azimuthal orientation accuracy of 2.45° in tracking the American football along the goal line. We noted some systematic errors that may allow calibrations to further increase the accuracy. Finally, the tests were conducted with a person obstructing one or more receivers at all times and with a persons hands directly on the ball (transmitter/emitter), thus illustrating the benefit of this approach in proximity to the human body.

## References

[1] D. Arumugam, J. Griffin, and D. Stancil, "Experimental Demonstration of Complex Image Theory and Application to Position Measurement," *IEEE Antennas Wireless Propag. Lett.*, vol. 10, pp. 282–285, April 2011.

[2] D. Arumugam, J. Griffin, D. Stancil, and D. Ricketts, "Three-Dimensional Position and Orientation Measurements using Magnetoquasistatic Fields and Complex Image Theory," *IEEE Trans. Antennas and Propogation*, submitted.

[3] ——, "Experimental study on the effects of groups of people on magnetoquasistatic positioning accuracy," *IEEE International Symp. on Antennas and Propag,*, pp. 1–2, July 2012.

[4] J. Weaver, "Image approximation for an arbitrary quasi-static field in the presence of a conducting half space," *Radio Science*, vol. 6, no. 6, pp. 647–653, June 1971.

[5] J. Jackson, "Classical Electrodynamics," John Wiley and Sons Inc., 1999.

[6] T. Coleman and Y. Li, "An interior trust region approach for nonlinear minimization subject to bounds," *SIAM Journal on Optimization*, vol. 6, no. 2, pp. 418–445, 1996.

[7] D. Arumugam, J. Griffin, D. Stancil, and D. Ricketts, "Two-dimensional position measurement using magnetoquasistatic fields," *Antennas and Propagation in Wireless Communications (APWC), 2011 IEEE-APS Topical Conference on*, pp. 1193–1196, Sept. 2011.

[8] MATLAB, *version 7.12.0 (R2011a)*. Natick, Massachusetts: The MathWorks Inc., 2011.

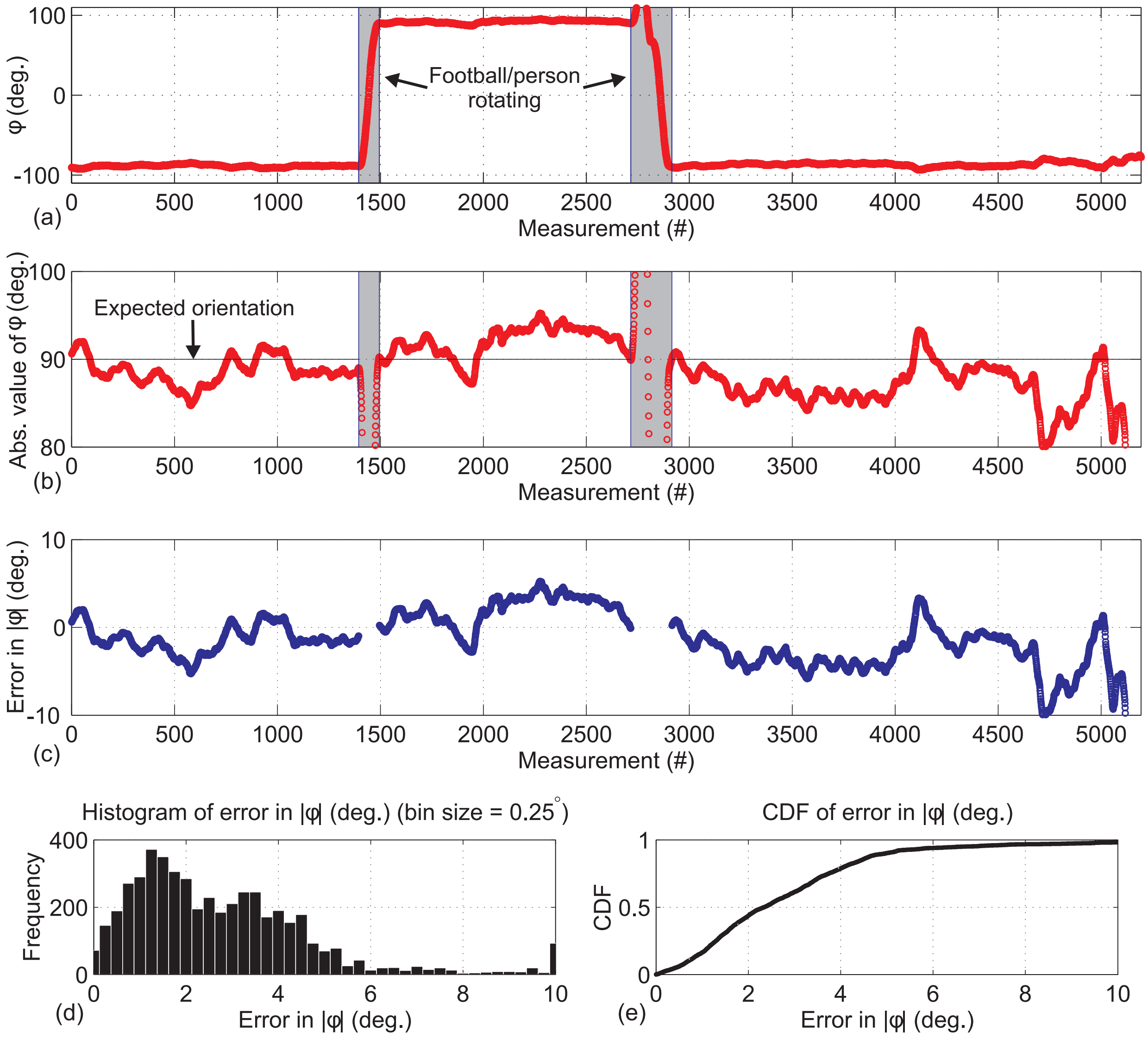


Fig. 7. Azimuthal orientation solutions from the measurements are shown in (a). The highlighted transition zones indicate regions where the person/football rotates. These occur at locations B and A in Fig. 6, respectively. The absolute value of the azimuthal orientation results are shown in (b). The purpose here is to allow a close-up view of the result. The estimated azimuthal orientation error is shown in (c). A histogram of the azimuthal orientation error is shown in (d). A CDF of the azimuthal orientation error is shown in (e).